Epitaxial graphene surface preparation for atomic layer deposition of Al_2O_3

N. Y. Garces,[1,2,a)] V. D. Wheeler,[2] J. K. Hite,[2] G. G. Jernigan,[2] J. L. Tedesco,[2] Neeraj Nepal,[2] C. R. Eddy Jr.,[2] and D. K. Gaskill[2]
[1]*Global Strategies Group, North America, 2200 Defense Hwy., Suite 405, Crofton, Maryland 21114, USA*
[2]*U.S. Naval Research Laboratory, 4555 Overlook Ave. SW, Washington, DC 20375, USA*

(Received 7 February 2011; accepted 30 April 2011; published online 20 June 2011)

Atomic layer deposition was employed to deposit relatively thick (~30 nm) aluminum oxide (Al_2O_3) using trimethylaluminum and triply-distilled H_2O precursors onto epitaxial graphene grown on the Si-face of silicon carbide. *Ex situ* surface conditioning by a simple wet chemistry treatment was used to render the otherwise chemically inert graphene surface more amenable to dielectric deposition. The obtained films show excellent morphology and uniformity over large (~64 mm^2) areas (i.e., the entire sample area), as determined by atomic force microscopy and scanning electron microscopy. X-ray photoelectron spectroscopy revealed a nearly stoichiometric film with reduced impurity content. Moreover, from capacitance-voltage measurements a dielectric constant of ~7.6 was extracted and a positive Dirac voltage shift of ~1.0 V was observed. The graphene mobility, as determined by van der Pauw Hall measurements, was not affected by the sequence of surface pretreatment and dielectric deposition. © *2011 American Institute of Physics*. [doi:10.1063/1.3596761]

INTRODUCTION

Graphene is an outstanding material for electronic device applications due to its exceptional electronic and physical properties, including high intrinsic carrier mobility, large thermal conductivity, and remarkable mechanical properties.[1–4] High-κ dielectrics such as Al_2O_3, HfO_2, Ta_2O_5, and TiO_2, are important for the realization of graphene-based top-gated electronic devices including field effect transistors (FETs), and to meet the challenge of scaling devices to small sizes (<100 nm). In addition, AlN is a suitable dielectric for epitaxial graphene (EG) due to the predicted reduced phonon scattering at the EG layer.[5] These dielectrics are envisioned to be thin (2–30 nm) with minimal trapped and mobile charges that otherwise would deleteriously affect device performance. They are also expected to enable operation at the very high frequencies needed for terahertz applications, to improve the channel mobility by screening charged impurities, and to have leakage currents below those observed in traditional silicon dioxide (SiO_2) gate oxides.[6]

Atomic layer deposition (ALD), a method based on two separate self-limiting surface reactions, is a preferred technique to achieve high-quality, conformal, ultra-thin dielectric films with precise thickness control.[7–9] Unfortunately, direct ALD of oxides on pristine or nonfunctionalized graphene sheets, using H_2O-based precursors, is hindered by the highly hydrophobic and chemically inert nature of graphene. Growth attempts on exfoliated graphene have led to no direct deposition on defect-free pristine exfoliated graphene.[10] On highly-oriented pyrolytic graphite (HOPG), as well as EG, ALD resulted in nonuniform coverage.[11,12] On exfoliated graphene and HOPG, ALD results in selective growth at the step edges and defects, where broken dangling bonds are believed to serve as nucleation sites for deposition.[13] For ALD on EG, preferential nucleation on terraces has been reported, yet nucleation along step edges is problematic.[12]

To render the graphene surface more suitable to oxide precursor bonding and/or to create a functionalized layer that will promote uniform deposition, several different surface preparation approaches have been investigated. Some of these approaches include: ozone (O_3) or nitrous oxide (NO_2) surface treatments of EG or HOPG;[12,14,15] initial ALD pulse sequencing of NO_2-trimethylaluminum (TMA);[16] oxidation of electron beam evaporated metallic Al, Hf, Ti, Ta;[17,18] and spin-coating of a buffered low-κ dielectric-seeding polymer.[19,20] These prior ALD approaches resulted in incomplete dielectric coverage and/or degradation of electronic properties of the underlying graphene. For example, some of the approaches altered the graphene surface, creating broken bonds and subsequently reducing mobility and degrading the performance of devices. Therefore, there remains a need to develop a viable method to deposit high-κ dielectrics on large area EG.

In this work, we present the results of four different wet chemical treatments on the surface of EG grown on the Si-face of SiC prior to ALD of Al_2O_3 films in promoting uniform, high quality oxide deposition. Initial treatments resulted in partial coverage, while the optimized treatment resulted in complete coverage and had negligible effects on the mobility of the underlying graphene. We used atomic force microscopy (AFM) and scanning electron microscopy (SEM) to monitor the surface morphology before and after oxide deposition, and x-ray photoelectron spectroscopy (XPS) to determine the chemical composition of the oxide. Sputter depth profiling was performed to observe compositional changes from the oxide to the EG interface and into the bulk of the SiC; this revealed a nearly stoichiometric oxide with reduced impurity content. Most importantly, the

[a)]Author to whom correspondence should be addressed. Electronic mail: nelson.garces@nrl.navy.mil.

Report Documentation Page

Form Approved
OMB No. 0704-0188

1. REPORT DATE	2. REPORT TYPE	3. DATES COVERED
JUN 2011		**00-00-2011 to 00-00-2011**

4. TITLE AND SUBTITLE	5a. CONTRACT NUMBER
Epitaxial Graphene Surface Preparation For Atomic Layer Deposition Of Al2O3	5b. GRANT NUMBER
	5c. PROGRAM ELEMENT NUMBER
6. AUTHOR(S)	5d. PROJECT NUMBER
	5e. TASK NUMBER
	5f. WORK UNIT NUMBER
7. PERFORMING ORGANIZATION NAME(S) AND ADDRESS(ES) **U.S. Naval Research Laboratory,4555 Overlook Ave. SW,Washington,DC,20375**	8. PERFORMING ORGANIZATION REPORT NUMBER
9. SPONSORING/MONITORING AGENCY NAME(S) AND ADDRESS(ES)	10. SPONSOR/MONITOR'S ACRONYM(S)
	11. SPONSOR/MONITOR'S REPORT NUMBER(S)

12. DISTRIBUTION/AVAILABILITY STATEMENT
Approved for public release; distribution unlimited

13. SUPPLEMENTARY NOTES
Journal of Applied Physics, Issue Date: Jun 2011, Volume: 109, Issue:12,page(s): 124304 - 124304-6

14. ABSTRACT
Atomic layer deposition was employed to deposit relatively thick (30 nm) aluminum oxide (Al2O3) using trimethylaluminum and triply-distilled H2O precursors onto epitaxial graphene grown on the Si-face of silicon carbide. Ex situ surface conditioning by a simple wet chemistry treatment was used to render the otherwise chemically inert graphene surface more amenable to dielectric deposition. The obtained films show excellent morphology and uniformity over large (64 mm2) areas (i.e., the entire sample area), as determined by atomic force microscopy and scanning electron microscopy. X-ray photoelectron spectroscopy revealed a nearly stoichiometric film with reduced impurity content. Moreover, from capacitance-voltage measurements a dielectric constant of 7.6 was extracted and a positive Dirac voltage shift of 1.0 V was observed. The graphene mobility, as determined by van der Pauw Hall measurements, was not affected by the sequence of surface pretreatment and dielectric deposition.

15. SUBJECT TERMS

16. SECURITY CLASSIFICATION OF:			17. LIMITATION OF ABSTRACT	18. NUMBER OF PAGES	19a. NAME OF RESPONSIBLE PERSON
a. REPORT **unclassified**	b. ABSTRACT **unclassified**	c. THIS PAGE **unclassified**	**Same as Report (SAR)**	**7**	

ALD oxide was found to have minimal impact on the electrical properties of the graphene.

EXPERIMENTAL DETAILS

Epitaxial graphene samples were grown by Si sublimation on the Si-face of 16×16 mm^2 semi-insulating, on-axis 6H-SiC substrates (II–VI, Inc.) in a commercial Aixtron VP508 chemical vapor deposition (CVD) reactor at temperatures ranging from 1580–1650 °C. Si-face samples were chosen as they have shown promise in RF field effect transistors.[21] The sublimation process took place in an Ar atmosphere at a constant pressure of 100 mbar for 1 h to 2.5 h. Additional details of the growth process can be found in Tedesco *et al.*[22] Samples prepared in this manner exhibited monolayer graphene on the terraces and 2 monolayers at SiC surface steps.[23] The samples were then cut into four 8×8 mm^2 coupons (A, B, C, and D) to form a standardized experimental set. To prevent surface contamination and protect the graphene from abrasion during cutting, Shipley-1818 photoresist was used. After cutting, the coupons were cleaned in an acetone bath at ~40 °C for 5 min, followed by a bath in isopropanol at ~40 °C for 5 min, and then rinsed with de-ionized water. All the coupons received this preliminary cleaning step before any other treatment was applied; and the presence or absence of residual photoresist was not verified, therefore, we consider their surfaces to be normalized at this stage.

We investigated the ability of four wet chemical treatments, listed in Table I, to enable uniform, high quality Al_2O_3 on EG by ALD. The HF portion in treatments II and IV was intended to remove any possible oxides and/or impurities from the graphene surface. The SC1 (Standard Clean 1) portion in treatments III and IV was expected to promote a hydroxyl-terminated graphene surface, thus improving reactivity with the trimethylaluminum (TMA) precursor during the initial ALD cycles. After each treatment was completed, the coupons were blown dry with N_2 and immediately placed in the ALD reactor for deposition. The reactor was preset at the desired deposition temperature and coupon loading resulted in a temperature decrease of ~3–4 °C that stabilized to the set point within ~4–6 min. To monitor the ALD process, p-type Si samples were placed alongside the graphene coupons. The Si witness samples were prepared using treatment IV, which was independently determined to be optimal for that surface.

The Al_2O_3 was deposited using a Cambridge NanoTech, Inc. Savannah 200 thermal ALD system. The sources were electronic-grade TMA (Sigma-Aldrich) and triply distilled H_2O which were both carried by N_2 (liquid nitrogen boil-off passed through a moisture filter). The experiments consisted of 250 cycles Al_2O_3 deposited at 200 °C on the graphene coupons, each having only one predeposition treatment as described in Table I. One ALD cycle consisted of the following precursor exposure and purging times: (i) 0.03 s TMA; (ii) 20 s N_2 purge; (iii) 0.03 s H_2O; (iv) 20 s N_2 purge. This sequence was independently verified to result in true ALD conditions with a saturated growth rate as defined elsewhere.[8] The N_2 carrier gas was set to 20 standard cubic centimeters per minute for the duration of the experiment and the base pressure in the reaction chamber was ~0.25 Torr. During TMA and H_2O exposures, the pressure increased to ~0.8 Torr. These conditions resulted in an average growth rate on Si witness samples of ~0.12 nm per cycle, which is typical for thermal ALD of Al_2O_3 at temperatures of ~200 °C.[24] Al_2O_3 was grown on coupons A, B, and C simultaneously; Al_2O_3 was grown on coupon D in a separate run with identical conditions to those of A, B, and C.

Sample morphology was characterized with a Veeco 3100 atomic force microscope (AFM) in tapping mode, and a LEO Supra 55 scanning electron microscope (SEM) with an in-lens detector. Variable angle spectroscopic ellipsometry (VASE) using a J.A. Woollam VASE system was employed to determine the thickness and refractive index of the oxide. Chemical composition of the oxide was determined using an Omicron Nanotechnology Sphera XPS system with monochromatic Al source x-rays ($h\nu = 1486.6$ eV). Photoelectrons from Si 2*p*, Al 2*p*, C 1*s*, and O 1*s* core levels were collected using a hemispherical analyzer with 50 eV pass energy. An acceptance aperture was used to permit only photoelectrons from a 1×1 mm^2 area within the sample to be accepted into the analyzer. The area was chosen to encompass the center of the sample and to avoid sample edge effects in the measurement. Sputter depth profiling for 420 min was accomplished using a 3 KeV Ar^+ ion beam rastered over a 5×5 mm^2 area. The angle of incidence for the ion beam was ~40°, and a beam current of 0.2 μA was used. This resulted in an effective sputter rate of ~0.07 nm min^{-1}. The system was calibrated by assigning the binding energy of Au $4f_{7/2}$ to 84.0 eV, and the adventitious carbon binding energy to 284.0 eV. The mobility of the graphene coupons

TABLE I. Different surface preparation treatments for epitaxial graphene prior to atomic layer deposition of Al_2O_3. Each coupon was subjected to one treatment only.

Treatment Name	Description	Coupon Identifier
I	No additional treatment after the cleaning step	A
II	a) Place in a (1:1) mixture of 49% hydrofluoric acid (HF) and 18.2 MΩ-cm deionized water (DI) for 1–2 min at room temperature. b) Rinse in DI water for approximately 1 min at room temperature.	B
III	a) Place in a SC1 solution (1 part 29% NH_4OH: 1 part 30% H_2O_2: 5 parts 18.2 MΩ-cm DI water) at 80 °C for approximately 10 min. b) Rinse in DI water for approximately 1 min. at room temperature.	C
IV	Treatment II followed by Treatment III.	D

before and after ALD was determined by van der Pauw Hall effect measurements using copper/beryllium point contacts in the four corners of the coupons. The dielectric constant and Dirac voltage were obtained from capacitance-voltage (C-V) measurements at 1 MHz on 50 μm diameter Ti/Au circular capacitors patterned on top of the oxide.

RESULTS AND DISCUSSION

Tapping mode AFM images taken in high resolution 9 μm^2 scans of coupons A, B, C, and D, after 250 cycles of Al_2O_3 deposition at 200 °C are shown in Figs. 1(a)–1(d), respectively. These images clearly show the impact of the different chemical treatments on the effectiveness of the ALD dielectric uniformity on the EG. First consider the deposition of Al_2O_3 after treatment I, shown in Fig. 1(a). This film was nonuniform, as evidenced by multiple pits with depths of ~8–12 nm on both the terraces and in particular on the step edges. The pit depth was less than the measured thickness of the oxide on the Si witness sample (~30 nm), suggesting an incubation period and nonuniform nucleation during ALD. The AFM rms roughness for this coupon was 1.64 nm.

Next, consider the deposition of Al_2O_3 after treatment II, shown in Fig. 1(b). Here we observe uniform deposition on the terraces but very wide pits in the vicinity of the step edges. Several pit depths were found to be ~ 30 nm, in agreement with the measured thickness from the Si witness sample thus demonstrating ALD growth on the terraces does not suffer from an incubation period as found in treatment I. The AFM-derived rms roughness for this coupon was 1.72 nm.

After treatment III, shown in Fig. 1(c), we also observe uniform deposition on the terraces, but areas of nonuniform nucleation are still found along the step edges. The film is smoother, with an AFM rms roughness of ~ 1.32 nm, and the pits are narrower than after treatment II. The pit depths are between 15–20 nm, thus indicating a varied incubation period and nonuniform nucleation. The nonuniform coverage of the oxide on the step edges in treatments I–III are attributed to variations in the chemical reactivity of bilayer graphene on the step edges as compared to that of monolayer graphene on the terraces, which is consistent with Speck *et al.*[12]

Figure 1(d) corresponds to the AFM morphology of coupon D deposited after treatment IV. This image shows morphology similar to that of the coupon before ALD deposition (not shown). In addition, the rms roughness of the coupon before and after the oxide deposition was 1.16 and 1.13 nm, respectively, implying the ALD did not impact this parameter. Since XPS verified the presence of Al_2O_3 (described below), the AFM image indicates conformal oxide coverage on both terraces and step edges without the presence of significant pits.

Figure 2 shows typical SEM images obtained from coupons A–D after ALD of Al_2O_3. It confirms the morphology details found in Fig. 1 on a larger scale (~80 μm^2). Coupons A–C clearly showed nonuniform Al_2O_3 films with pitted areas on the terraces and in the vicinity of step edges. In contrast, the SEM scan of coupon D shown in Fig. 2(d), indicates a uniform, continuous film across the step edges and terraces without interruptions. Since this was the only successful treatment for uniform, conformal Al_2O_3 deposition, the remainder of this paper will discuss the results on coupon D alone. Similar results to those on coupon D were obtained in subsequent experiments under identical conditions.

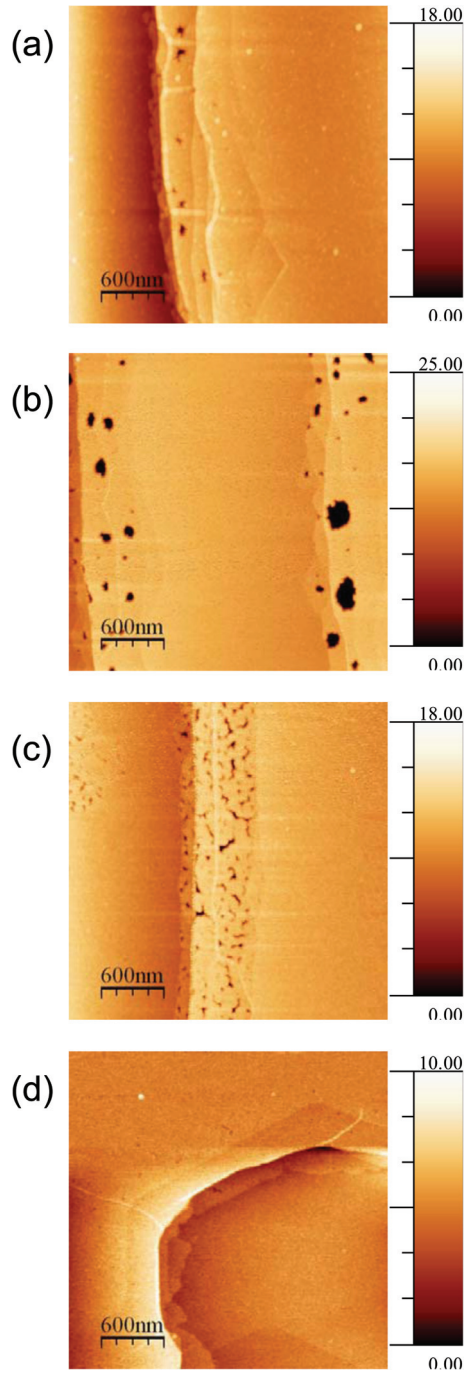

FIG. 1. (Color online) AFM images (9 μm^2) of coupons A, B, C, and D after 250 cycles Al_2O_3 ALD deposited at 200 °C. (a) Coupon A after treatment I, (b) Coupon B after treatment II, (c) Coupon C after treatment III, and (d) Coupon D after treatment IV. Coupons A–C show nonconformal deposition with multiple pits on the terraces and step edges, whereas coupon D shows conformal coverage. The vertical scale is in nanometers for all images.

Independent XPS studies revealed compositional changes to the EG surface after each step of the optimized treatment IV prior to oxide deposition. Results confirm that treating SiC/EG samples with HF reduces the total preexisting O content, although some carbonyl groups remain on the

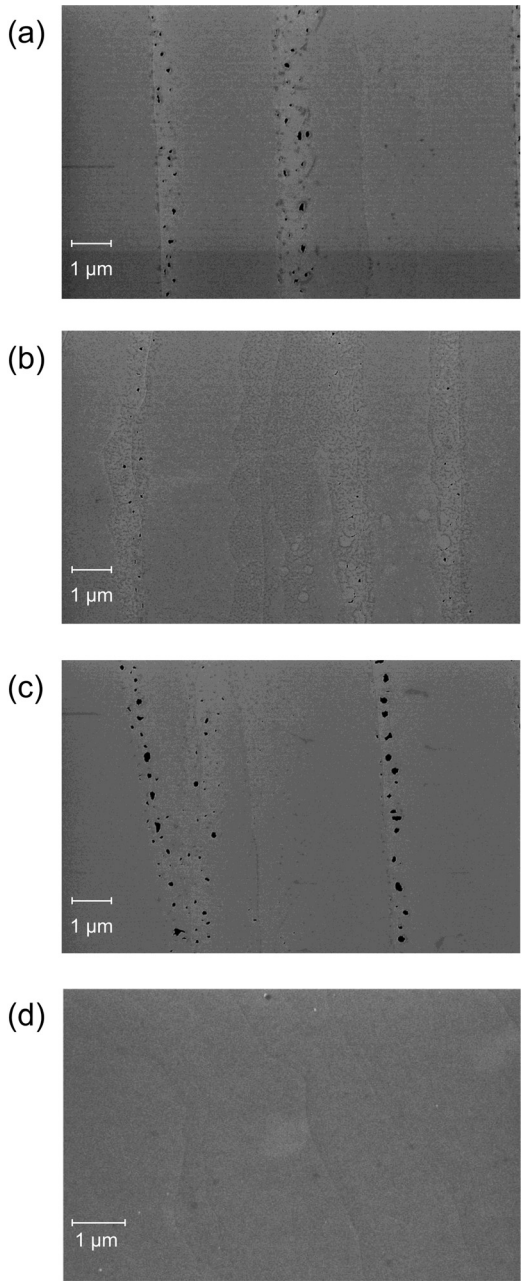

FIG. 2. SEM images obtained from an ~80 μm^2 area of Coupons A–D after 250 ALD cycles Al_2O_3 at 200 °C. (a)–(c) correspond to coupons A–C after treatments I, II, and III, respectively. The nonuniform coverage of the oxide is evident in this larger scale. (d) Coupon D shows that complete Al_2O_3 coverage was achieved after treatment IV.

surface. Moreover, the subsequent SC1 treatment further reduces the O and carbonyl content, as well as leaving ~4% O-H surface bonds, which act as additional nucleation sites needed for uniform ALD films. These findings verify the assumptions stated in the experimental section.

Chemical analysis of the oxide grown on coupon D was obtained from XPS peak positions and peak areas for the O 1*s*, Al 2*p*, and C 1*s* photoelectrons. Figures 3(a)–3(c) show the XPS spectra of the O 1*s*, Al 2*p*, and C1*s* peaks, respectively, after the initial 20 mins of sputtering through the oxide (approximately 1.4 nm into the film). Analysis of this data indicates that the oxide grown on the EG was nearly stoichiometric Al_2O_3. Correcting for the different experimental cross sections of the Al 2*p* and O 1*s*, this ratio is equivalent to an O/Al ratio of 1.57, comparable to XPS spectra taken of a single crystal sapphire standard. The O 1*s* line, centered about 532.18 eV, appears to have a slight asymmetry. Deconvolution of the peak reveals two distinct components, one at lower energy centered about 532.20 eV, participating in Al-O bonding, and one slightly shifted toward higher energy at 533.90 eV, associated with Al-O-H hydroxyl groups resulting from the ALD process with TMA/H_2O.[25,26] The Al 2*p* is a single symmetric line centered about 75.38 eV. The binding energy separation between the O 1*s* and Al 2*p* core levels is ~456.80 eV, in agreement with reported values for fully oxidized amorphous aluminum oxide.[25,27] The C 1*s* spectrum is shown in Fig. 3(c). This very small peak near 283.2 eV is most likely residual carbon from incomplete precursor reactions within or near the surface of the dielectric. Although the O/Al ratio and presence of hydroxyl groups indicate a slight O enrichment in the oxide, the narrow full-width at half maximum of the O 1*s* (1.93 eV) and Al 2*p* (1.6 eV) peaks as well as the small amount of residual carbon in the film are indicative of a high quality oxide. Post-growth processing (e.g., post oxidation anneals) and variable pulse sequencing are being explored to further improve the oxide resulting from the ALD growth process.

Sputter depth profiling was performed to determine if the composition and chemical nature of the films changed from the oxide surface to the oxide/graphene interface. Figure 4 plots the peak areas of Al 2*p*, O 1*s*, Si 2*p*, and C 1*s* as a function of sputtering time for coupon D. A sputtering time of 0 min corresponds to the surface of the oxide, while 420 min corresponds to the SiC bulk, i.e., all the oxide and EG have been removed. The Si and C signals from the interfacial region between the SiC/EG and Al_2O_3 can be observed even though ~11 nm of the oxide remains. This is due to the long electron escape depth of Si 2*p* and C 1*s* through the oxide, which is consistent with similar observations on other oxides such as SiO_2 grown on SiC.[28] In summary, XPS conclusively demonstrated that a near-stoichiometric, reduced carbon impurity Al_2O_3 film was deposited throughout by thermal ALD on Si-face EG subjected to treatment IV.

The Hall mobility of coupon D was not significantly affected by either the predeposition treatment or the Al_2O_3 deposition, as only a small change was observed from ~550 $cm^2\ V^{-1}s^{-1}$ before ALD to ~600 $cm^2\ V^{-1}s^{-1}$ after ALD. This amounts only to ~10% change which is within the experimental error of the measurement. It has been argued that electrical measurements are a highly sensitive indicator of minute changes in the quality of the EG, whereas techniques such as Raman spectroscopy are used to evaluate larger scale variations.[29] Since the mobility of coupon D was maintained, this implies that the graphene structure is not significantly deteriorated by the optimized surface treatment and the oxide deposition. Unlike the mobility, the sheet carrier density increased from -8.9×10^{11} cm^{-2} before ALD to -1.1×10^{13} cm^{-2} after ALD. Lin *et al.*[30] proposed that the outermost layer of EG grown on the C-face of SiC is doped heavily p-type. In addition, Lohmann *et al.*[31] also presented data supporting the mechanism of adsorbed water causing the surface of graphene to be p-type. Thus, it seems likely that the

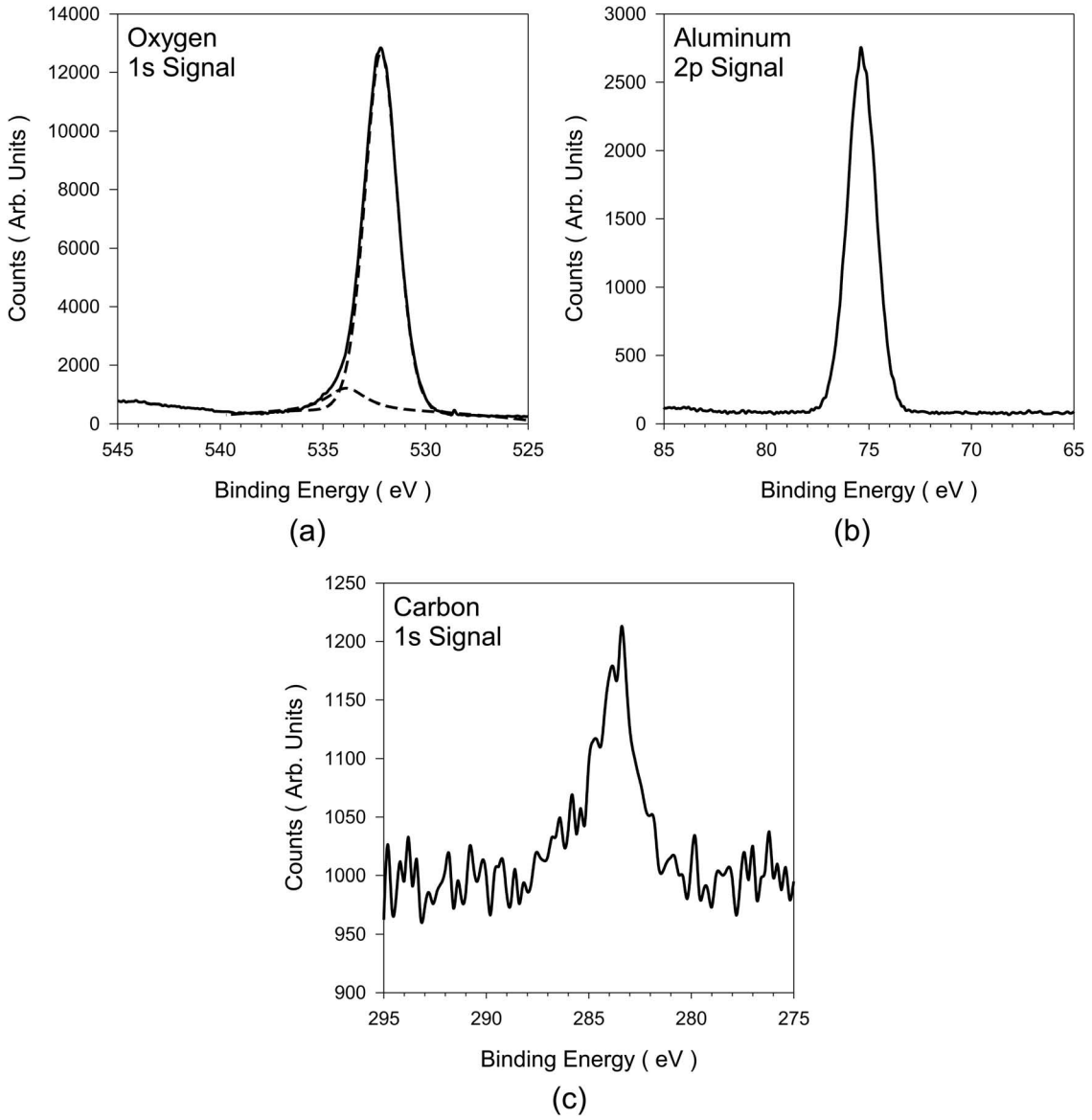

FIG. 3. XPS spectra from Coupon D recorded after 20 min sputtering (~1.4 nm depth) through the Al_2O_3 layer. (a) O 1*s* peak, (b) Al 2*p* peak, and (c) C 1*s* peak. The O 1*s* spectrum is fitted with two lines separated by ~1.7 eV.

cause of the increased doping is due to the removal of compensating p-type environmental factors either by the chemical treatment or subsequent ALD. The significant increase in sheet carrier density without a significant change in the mobility after the ALD process is interesting, yet not fully understood, and is currently under investigation.

A capacitance-voltage measurement on coupon D, shown in Fig. 5, resulted in a Dirac voltage of ~1.0 V. Using the measured 31 nm dielectric thickness, a dielectric constant of ~7.6 was extracted. The Si witness samples confirmed the thickness (~30.1 ± 0.8 nm), but produced a more ideal dielectric constant of ~8.7–9.0. The lower dielectric constant on coupon D may be the result of hydroxides and carbon trapped within the oxide. Theoretical investigations on metal-oxide-graphene capacitance predict that even without any source doping, the Dirac voltage can be nonzero, solely due to the relative band offsets of the metal to oxide and semiconductor/graphene to oxide. Also, fixed charge in the substrate, in the oxide, or at the graphene-substrate/graphene-oxide interface can result in a shift of the Dirac voltage, but quantities in excess of $\geq 10^{12}$ cm^{-2} are required to appreciably shift ($\geq$1 V) the Dirac voltage.[32] Thus, the C-V measurements imply a relatively low charge density in the Al_2O_3.

CONCLUSIONS

We have demonstrated that relatively thick (~30 nm) conformal uniform and high quality Al_2O_3 films can be deposited on Si-face EG using a simple wet chemical surface treatment prior to thermal ALD. The film purity probed by XPS showed minimal carbon contamination and excellent stoichiometry. Therefore, we conclude that treatment IV, involving sequential use of HF followed by SC1 has rendered the otherwise chemically inert graphene surfaces more suitable to ALD growth of Al_2O_3 using TMA and H_2O precursors. Also, the underlying graphene mobility was maintained, indicating minimal impact by the chemical treatment

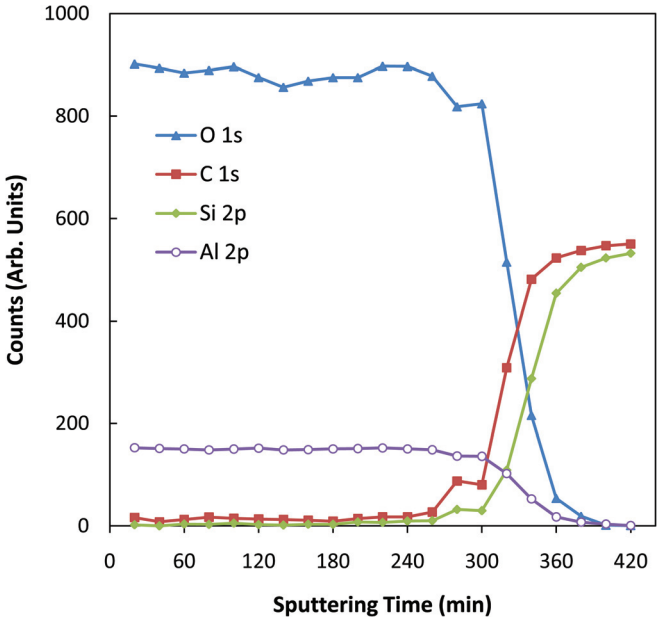

FIG. 4. (Color online) XPS peak areas for O 1*s*, Al 2*p*, C 1*s*, and Si 2*p* as a function of sputtering time for Al_2O_3 deposited by ALD on Si-face epitaxial graphene.

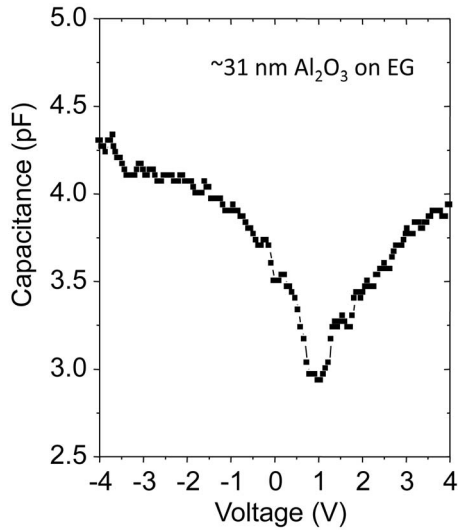

FIG. 5. C-V measurement at 1 MHz from a 50 μm diameter Ti/Au circular capacitor patterned on coupon D.

or ALD process. The sheet charge density was found to increase significantly, yet this result is consistent with the chemical treatment/ALD process removing compensating environmental factors from the surface of the EG. From the C-V measurement a dielectric constant of ~7.6 was extracted, and the measurement yielded a Dirac voltage of ~1.0 V, which are both indicative of device quality oxide. Further work, such as post oxidation anneals, may result in more ideal C-V characteristics and film composition.

ACKNOWLEDGMENTS

The authors thank Paul E. Sheehan for kindly providing access to his spectroscopic ellipsometer and for helpful suggestions fitting the data. J.L.T., V.D.W., and J.K.H. acknowledge the support of the American Society for Engineering Education Naval Research Laboratory Postdoctoral Fellowship Program. Work at the U.S. Naval Research Laboratory is supported by the Office of Naval Research.

[1]K. S. Novoselov, A. K. Geim, S. V. Morozov, D. Jiang, Y. Zhang, S. V. Dubonos, I. V. Grigorieva, and A. A. Firsov, Science **306**, 666 (2004).
[2]K. S. Novoselov, A. K. Geim, S. V. Morozov, D. Jiang, M. I. Katsnelson, I. V. Grigorieva, S. V. Dubonos, and A. A. Firsov, Nature **438**, 197 (2005).
[3]A. K. Geim and K. S. Novoselov, Nature Mater. **6**, 183 (2007).
[4]C. Lee, X. D. Wei, J. W. Kysar, and J. Hone, Science **321**, 385 (2008).
[5]A. Konar, T. A. Fang, and D. Jena, Phys. Rev. B **82**, 115452 (2010).
[6]Q. Lu, D. Park, A. Kalnitsky, C. Chang, C. C. Cheng, S. P. Tay, T. J. King, and C. M. Hu, IEEE Electron Device Lett. **19**, 341 (1998).
[7]T. Suntola, Mater. Sci. Rep. **4**, 261 (1989).
[8]S. M. George, A. W. Ott, and J. W. Klaus, J. Phys. Chem. **100**, 13121 (1996).
[9]R. L. Puurunen, J. Appl. Phys. **97**, 121301 (2005).
[10]X. R. Wang, S. M. Tabakman, and H. J. Dai, J. Am. Chem. Soc. **130**, 8152 (2008).
[11]L. Bongki, P. Seong-Yong, K. Hyun-Chul, C. KyeongJae, E. M. Vogel, M. J. Kim, R. M. Wallace, and K. Jiyoung, Appl. Phys. Lett. **92**, 203102 (2008).
[12]F. Speck, M. Ostler, J. Rohrl, K. V. Emtsev, M. Hundhausen, L. Ley, and T. Seyller, Phys. Status Solidi C **7**, 398 (2010).
[13]Y. Xuan, Y. Q. Wu, T. Shen, M. Qi, M. A. Capano, J. A. Cooper, and P. D. Ye, Appl. Phys. Lett. **92**, 013101 (2008).
[14]B. Lee, G. Mordi, T. J. Park, L. Goux, Y. J. Chabal, K. J. Cho, E. M. Vogel, M. J. Kim, L. Colombo, R. M. Wallace, and J. Kim, ECS Trans. **19**, 225 (2009).
[15]D. B. Farmer and R. G. Gordon, Nano Lett. **6**, 699 (2006).
[16]Y. M. Lin, K. A. Jenkins, A. Valdes-Garcia, J. P. Small, D. B. Farmer, and P. Avouris, Nano Lett. **9**, 422 (2009).
[17]A. Pirkle, R. M. Wallace, and L. Colombo, Appl. Phys. Lett. **95** (2009).
[18]J. A. Robinson, M. LaBella, K. A. Trumbull, X. J. Weng, R. Cavelero, T. Daniels, Z. Hughes, M. Hollander, M. Fanton, and D. Snyder, ACS Nano **4**, 2667 (2010).
[19]D. B. Farmer, H. Y. Chiu, Y. M. Lin, K. A. Jenkins, F. N. Xia, and P. Avouris, Nano Lett. **9**, 4474 (2009).
[20]C. Dimitrakopoulos, Y. M. Lin, A. Grill, D. B. Farmer, M. Freitag, Y. N. Sun, S. J. Han, Z. H. Chen, K. A. Jenkins, Y. Zhu, Z. H. Liu, T. J. McArdle, J. A. Ott, R. Wisnieff, and P. Avouris, J. Vac. Science. Technol. B **28**, 985 (2010).
[21]J. S. Moon, D. Curtis, S. Bui, M. Hu, D. K. Gaskill, J. L. Tedesco, P. Asbeck, G. G. Jernigan, B. L. VanMil, R. L. Myers-Ward, C. R. Eddy, P. M. Campbell, and X. Weng, IEEE Electron Device Lett., **31**, 260 (2010).
[22]J. L. Tedesco, G. G. Jernigan, J. C. Culbertson, J. K. Hite, Y. Yang, K. M. Daniels, R. L. Myers-Ward, C. R. Eddy, J. A. Robinson, K. A. Trumbull, M. T. Wetherington, P. M. Campbell, and D. K. Gaskill, Appl. Phys. Lett. **96**, 222103 (2010).
[23]J. A. Robinson, M. Wetherington, J. L. Tedesco, P. M. Campbell, X. Weng, J. Stitt, M. A. Fanton, E. Frantz, D. Snyder, B. L. VanMil, G. G. Jernigan, R. L. Myers-Ward, C. R. Eddy, and D. K. Gaskill, Nano Lett. **9**, 2873 (2009).
[24]E. Langereis, S. B. S. Heil, H. C. M. Knoops, W. Keuning, M. C. M. van de Sanden, and W. M. M. Kessels, J. Phys. D **42**, 073001 (2009).
[25]O. Renault, L. G. Gosset, D. Rouchon, and A. Ermolieff, J. Vac. Sci. Technol. A **20**, 1867 (2002).
[26]M. R. Alexander, G. E. Thompson, and G. Beamson, Surf. Interface Anal. **29**, 468 (2000).
[27]J. van den Brand, P. C. Snijders, W. G. Sloof, H. Terryn, and J. H. W. de Wit, J. Phys. Chem. B **108**, 6017 (2004).
[28]G. G. Jernigan, R. E. Stahlbush, and N. S. Saks, Appl. Phys. Lett. **77**, 1437 (2000).
[29]R. R. Nair, W. Ren, R. Jalil, I. Riaz, V. G. Kravets, L. Britnell, P. Blake, F. Schedin, A. S. Mayorov, S. Yuan, M. I. Katsnelson, H. M. Cheng, W. Strupinski, L. G. Bulusheva, A. V. Okotrub, I. V. Grigorieva, A. N. Grigorenko, K. S. Novoselov, and A. K. Geim, Small **6**, 2877 (2010).
[30]Y. M. Lin, C. Dimitrakopoulos, D. B. Farmer, S. J. Han, Y. Q. Wu, W. J. Zhu, D. K. Gaskill, J. L. Tedesco, R. L. Myers-Ward, C. R. Eddy, A. Grill, and P. Avouris, Appl. Phys. Lett. **97**, 112107 (2010).
[31]T. Lohmann, K. von Klitzing, and J. H. Smet, Nano Lett. **9**, 1973 (2009).
[32]J. G. Champlain, private communication (2011).